

**LOW TEMPERATURE ULTRAVIOLET LAMP-ASSISTED
PHOTOETCHING OF GaAs**

Diane L. Miller
B.A., Mount Holyoke College, Massachusetts, 1986

A thesis submitted to the faculty
of the Oregon Graduate Center
in partial fulfillment of the
requirements for the degree
Master of Science
in
Applied Physics

July, 1989

The thesis "Low Temperature Ultraviolet Lamp-Assisted Photoetching of GaAs" by Diane L. Miller has been examined and approved by the following Examination Committee:

R. Solanki, Thesis Research Advisor
Associate Professor

P. Kirk Boyer, Ph. D.
Tektronix, Inc.

Paul R. Davis
Professor

ACKNOWLEDGEMENTS

I am greatly indebted to Jack Sachitano and the Solid State Research Laboratory group of Tektronix for supporting this thesis. In addition to their financial and material assistance, I would like to thank Dr. P. Kirk Boyer for his willing advice and guidance. Bob Herman, Curtis Haynes, Jan Bowman, Janeen Castillo, and many others also deserve tremendous thanks for their help and friendship while this work was underway at Tektronix.

I am very grateful for the endless patience and encouragement that my advisor, Dr. Raj Solanki offered me. Thanks, too, to Dr. Paul Davis for his willing participation on my examination committee.

Not to be forgotten, I wish to mention my gratitude to Dr. Dave Lishan at the University of California - Santa Barbara for his suggestions and help in analysis of the data. Also thanks to Dr. Mike Bozack for his generosity in contributing his time for the Auger analysis of my samples.

For my mentor, Dr. Howard Nicholson

Table of Contents

LIST OF FIGURES	vi
LIST OF TABLES	vii
ABSTRACT	viii
I. INTRODUCTION	1
II. EXPERIMENT	5
III. RESULTS	9
IV. DISCUSSION	30
V. CONCLUSION	42
REFERENCES	44
BIOGRAPHICAL NOTE	47

LIST OF FIGURES

1	Schematic diagram of experimental equipment	6
2	Spectral output of the lamp between 200 and 450 nm with a superimposed plot (dotted line) of the absorption coefficients of chlorine, reprinted from <i>Okabe</i> ¹²	10
3	Lateral distribution of the beam power as a function of distance from the lamp	11
4	Temperature dependence of GaAs photoetch: experiments with 80 sccm chlorine and chamber pressure of 4 torr	13
5	Arrhenius plot of 80 sccm chlorine, 4 torr, thermal etch of GaAs	15
6	Arrhenius plot of 80 sccm chlorine, 4 torr, photoetch of GaAs	16
7	Dependence of GaAs photoetch upon chamber pressure of chlorine: experiments were run for constant temperatures of 25, 50, 100 °C	17
8	Auger spectroscopic analysis of surfaces of GaAs substrates (A,B,C,D) in progressive stages of an experimental run	22
9	Photon dependence of GaAs photoetch: experiments at 50 °C and chamber pressures of 0.8 and 6.0 torr chlorine	24
10	SEM micrograph showing the smooth-walled profile of low speed etches	27
11	SEM micrograph showing the crystallographic etching of high speed etches	28
12	SEM micrograph showing the etch trenching feature parallel to the edge of the GaAs mask	29
13	Arrhenius plots of the etch rate versus 1000/T (in degrees Kelvin) for the following chamber pressures: 0.5, 1.0, 2.0, 6.0 torr	39

LIST OF TABLES

1	Chemical dependence of GaAs photoetch: experiments with chlorine and oxygen as etchant gases	19
2	Chemical dependence of GaAs photoetch: experiments with chlorine and argon as etchant gases	21
3	Substrate effect in GaAs photoetch: experiments with Horizontal-Bridgeman (HB) grown, $\langle 100 \rangle$ n-type GaAs of doping density 10^{18} cm^{-3} , and liquid encapsulated Czochralski (LEC) grown, $\langle 100 \rangle$ GaAs with an n-type doping density of 10^{17} cm^{-3}	26
4	Calculated values for the ratio of transmitted lamp intensity reaching the substrate surface for a chlorine pressure range of 0.5 to 8.0 torr	31
5	Calculated values for the volume per molecule and mean free path of Cl_2 for varying pressures	33
6	Calculated values for the residence time of Cl_2	35
7	Activation energies of GaAs photoetch for a range of chlorine pressures, derived from Arrhenius plots of the etch rate versus $1000/T$ (in degrees Kelvin)	40

ABSTRACT

LOW TEMPERATURE ULTRAVIOLET LAMP-ASSISTED
PHOTOETCHING OF GaAs

Diane L. Miller

Oregon Graduate Center, 1989

Supervising Professor: Dr. Raj Solanki

Plasma etching currently is used widely in fabrication of very large scale integrated (VLSI) devices because of its valuable directional etching. This process, however, creates crystal structure damage which could be avoided if a less energetic process were utilized.

This thesis explored the feasibility of a uv lamp assisted etch which because of its photochemical mechanism would avoid the radiation damage problems of the energetic plasma etch process. Using low pressures of Cl_2 , low temperatures, and uv lamp irradiation, etch rates of GaAs were measured with respect to changes in Cl_2 pressure, substrate temperature, lamp intensity, and doping level of the substrate. Etch rates were obtained from 10 Å/min to 10 μm/min. Analysis of experimental data revealed that all etch reactions occurring at $>25^\circ C$ were driven by a thermal mechanism; only etching occurring at $\leq 25^\circ C$ had a photochemical component. However, this latter reaction was found to be non-reproducible. This did not appear to be due to contamination, but rather to the desorption of $GaCl_3$.

I. INTRODUCTION

Very large scale integrated (VLSI) devices are microcircuits fabricated from semiconductor materials by a series of processes which include thin film deposition, oxidation, ion implantation, and etching. Etching methods are important to device fabrication since the selective removal of semiconductor material allows VLSI features like vias between separated layers and isolation of device regions. Of the etching techniques, the original wet chemical etch used for the fabrication of microcircuit features has been largely replaced by sputter assisted etching processes. This new plasma technology, unlike liquid etchants, avoids the problems of undercutting of the microcircuit layers by capillary action, isotropic or nondirectional etching, and of inexact etch exposures due to wet chemicals clinging to the semiconductor materials after removal from the etch solution.¹

Plasma etching is a dry process; the semiconductor material is surrounded by an ionized gas - a plasma - and etching occurs from both chemical reactions and physical bombardment of the surface. The etchant gases are ionized by an electrical discharge and due to the electric fields inherent to the discharge within the reaction chamber, the generated ions are directional. This results in a directional or anisotropic etch which is more valuable for VLSI device processing than the undercutting action of wet chemical etches. Plasma etching also is inherently more controllable since etching stops instantaneously when the electrical discharge is discontinued. The only serious disadvantage of this etching, however, is that it creates surface damage to the crystal structure. This is a problem since crystal damage translates

directly into poor performance of the semiconductor device. ²

Therefore, in the interest of eliminating this problem, two types of approaches have been undertaken. One method is to modify the plasma process. This could be accomplished either by changing the chemistry of the reaction or by localizing the ion bombardment. ^{3,4} The second approach to the problem of plasma induced damage is to discover a new method.

In hopes of finding a process with only the benefits of plasma etching, photochemical etching has been explored. ^{5,6} Photochemical reactions define all those reactions with photon interaction. The photons can excite reactants which then chemically attack the substrate surface, or can excite the surface of the substrate overcoming an activation energy barrier, or both. In the case of surface activation, the chemical etch would only occur on those surfaces exposed to the radiation, where the activated gaseous species exist, so that anisotropic etching would result due to the shadow effect. There is no particle nor ion bombardment of the surface so the resulting process potentially creates very little surface damage. Therefore unless very high energy photons are used, the damage problems of plasma processing could be overcome.

The possibility of a photochemical etch process has interested many research groups⁷⁻⁹ and all have demonstrated its feasibility with varying degrees of success. For example, Horiike, et. al¹⁰ , photochemically etched silicon with chlorine in an ultraviolet light-excited process, generating the uv photons with an excimer laser. They found etch rates of n-type silicon up to 0.3 $\mu\text{m}/\text{min}$ and the technique was anisotropic. Similarly, Brewer, et. al¹¹ , used an excimer laser to activate gaseous methyl halides, generating etch

rates of GaAs up to 1 $\mu\text{m}/\text{min}$ and found it to yield high anisotropy and smooth surfaces. Ashby¹² activated Cl_2 gas in a plasma then sent it downstream to the substrate. She found that GaAs was very reactive with this chlorine species when the substrate surface was irradiated with 514 nm photons from a focussed Ar^+ laser. Most importantly, she found that this reaction was exclusively photochemical. By comparing an Arrhenius plot of her data with an Arrhenius plot of a thermal reaction, she reported that there was absolutely no correlation between the two. This forced the conclusion that the etching reaction was photochemical. A more recent study by Ikawa, et. al¹³, demonstrated that photoetching of silicon in chlorine gas could be achieved with an ultraviolet lamp. This development was particularly interesting since the replacement of a lamp for a laser would be much more efficient and economical for VLSI processing. While a laser can generate high intensities when focussed to a spot, a high power lamp is a broad beam source and therefore exposes a much greater area. This allows a larger throughput making a lamp much more economical to operate.

In another attempt to find a photochemical etch process, this study was undertaken. Due to the sponsors' interest in the applications of GaAs for optoelectronics, GaAs was chosen as the subject of the study. In hopes of discovering a simple photochemical etch process, a system was designed featuring low temperatures, low vacuum pressure, chlorine gas, and an ultraviolet lamp. This was expected to induce minimal or no thermal damage to the soft semiconductor material, yield anisotropic etching with high etch rates, avoid any outdiffusion of As occurring at high temperatures, and be economical by only requiring a low vacuum pumping system and using a

broad beam lamp rather than a laser. What follows is a description of this experiment design in chapter 2, then a presentation of results in chapter 3, analysis of those results in chapter 4, and conclusions about the process in chapter 5.

II. EXPERIMENT

A reaction chamber to explore this uv lamp assisted etching process needed to be developed. The experimental system used is diagrammed in Figure 1. The reaction chamber was constructed from uv-transparent quartz and was evacuated with a rotary pump-roots blower combination from Leybold Hereaus capable of obtaining a background pressure of just under 1 mtorr. A stainless steel water cooled sample mount was installed inside the chamber with an inset thermocouple junction on its front face. Type K thermocouple wires were used to eliminate corrosion from the etchant gases. Etchant and purge gases were inlet through mass-flow controllers. Chamber pressure was controlled by a throttle valve on the outlet pumping line.

The light source was a microwave excited mercury lamp from Fusion Systems, Inc., model # F450-10. Light from its 10 inch long bulb was collimated along the direction of the bulb and focussed to a point 3 inches from the front of the lamp. A deionized water filter was constructed and placed in the light path, in order to filter out radiation of wavelengths greater than $1\mu\text{m}$. Water flowed through the 3 cm thick filter at a rate of 10 gph.

Samples approximately 0.5 cm by 0.5 cm were cleaved from 2 inch wafers of n-type, (100) GaAs. Before etching, the samples were cleaned in 3:1 HF acid solution, rinsed in deionized water, dried with N_2 and then adhered to the sample mount surface, directly over the thermocouple junction. A variety of adhesives were tested: melted indium adhered very well and provided excellent thermal conductivity but its use was awkward and

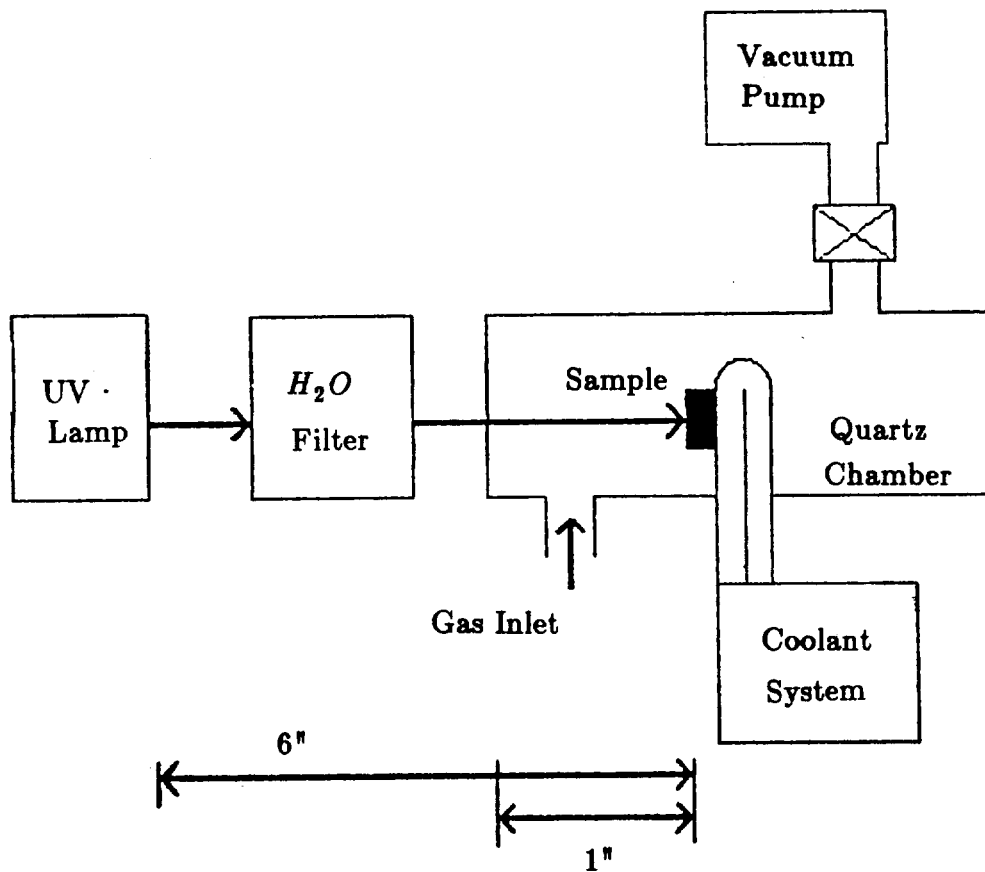


Figure 1. Schematic diagram of experimental equipment.

time-consuming. Colloidal silver paint also yielded excellent heat conductance, however these samples were difficult to remove once mounted. Finally, a colloidal black carbon paint (DAG) in a water based solution was used. It had good thermal conductivity, adhered samples well and was easy to apply and remove.

In order to determine the depth and profiles of the samples after etching, a stripe pattern contact mask was placed over the substrate surface. A variety of thin film masks were tested. Patterned photoresist masks were used originally, however, these lost integrity and flowed over the entire sample whenever the substrate was heated to more than 50°C under uv irradiation. Next, a deposited layer of SiO_2 was etched (reactive ion etching) into a stripe pattern mask. These masks held up under the experimental conditions, however, such substrate samples evidenced a loading effect - a noticeable drop in the reaction rates. In subsequent batches of these prepared substrates, though, problems with the consistency of the oxide mask layer arose. The final solution was to use a mask layer of plasma deposited silicon nitride. Upon testing, this mask of SiN_x was found to exhibit no measurable etching either when cleaned with HF or when subjected to the experimental conditions.

Within the experimental chamber, an inset thermocouple junction on the sample mount measured the temperature of the sample during all processes. By changing the coolant system from a water bath to heated nitrogen, the substrate temperature was set at any temperature in the range of 10°C to 200°C.

The concentration and ratios of inlet gases were regulated by mass-flow controllers (which were calibrated regularly to insure accuracy) and the experiment chamber pressure was controlled either by automatic throttle valve on the outlet to the roughing pump, or by manual adjustment of the valve position. All experiments were conducted with chlorine as the etchant gas.

Before and after etching, the step height of the mask of all samples was measured by a surface profiler. The surface profiler used was a Tencor Instruments α -step with an accuracy to $\pm 5\text{\AA}$. The etch rate of the sample was calculated by dividing the measured etched depth (ie. the change in step height) by the elapsed time for etching. In order to characterize the etched profiles resulting from different experiment conditions, cross-sectional scanning electron micrographs were taken.

III. RESULTS

In this section, experimental results will be presented in the approximate order of their completion. The first task was to characterize the lamp to be used as a light source and then begin etching experiments. The overall plan was to explore the temperature and pressure dependence of this chlorine etch first, and then determine the photon and chemical dependences.

Characterization of the lamp emission was done with both a spectrometer and a power meter. The power meter used was a Coherent model 201 with a 1 cm^2 thermal disc in a small detector head. This detector measured the power generated between 300 nm and $30 \text{ }\mu\text{m}$ with an accuracy of $\pm 1\%$. Figure 2 gives the spectral output of the ultraviolet lamp from Fusion Systems, Inc. As detailed by the lamp manufacturer, most of the lamp's power is derived from the wavelengths shorter than 450 nm, so no measurements were made of the lamp for wavelengths greater than 450 nm. Additionally, the photon absorption of chlorine (see Figure 2) peaks at 340 nm and drops to near zero by 400 nm so that wavelengths greater than 450 nm would not have significant effect upon the chlorine molecule. The longer wavelengths would cause heating of the substrate which was measured with the installed thermocouple.

Figure 3 shows the lateral distribution of the beam power as a function of distance from the lamp. At three inches from the lamp bulb, the light was focussed in a tight, vertical column. At five inches from the bulb, the light had diverged to form two intensity peaks separated by almost one inch. At seven inches from the bulb, the light clearly had reduced intensity and

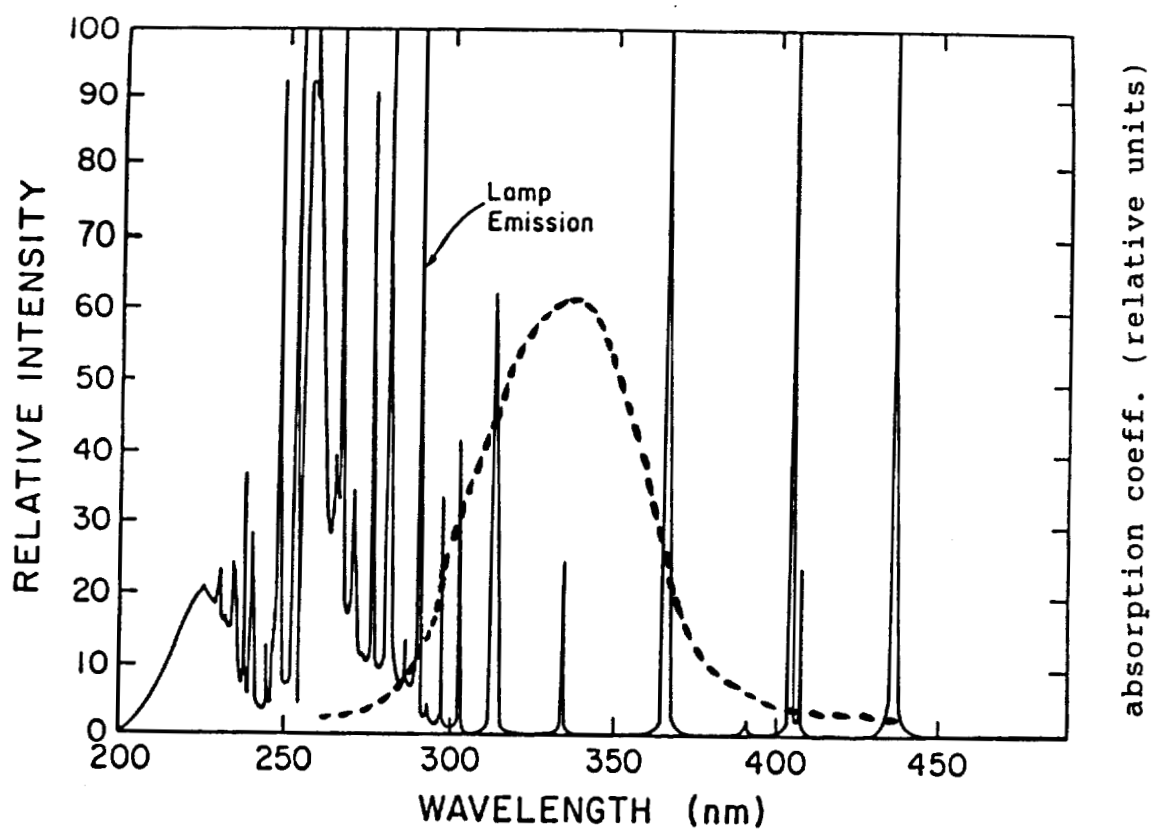


Figure 2. Spectral output of the lamp between 200 and 450 nm with a superimposed plot (dotted line) of the absorption coefficients of chlorine, reprinted from Okabe¹².

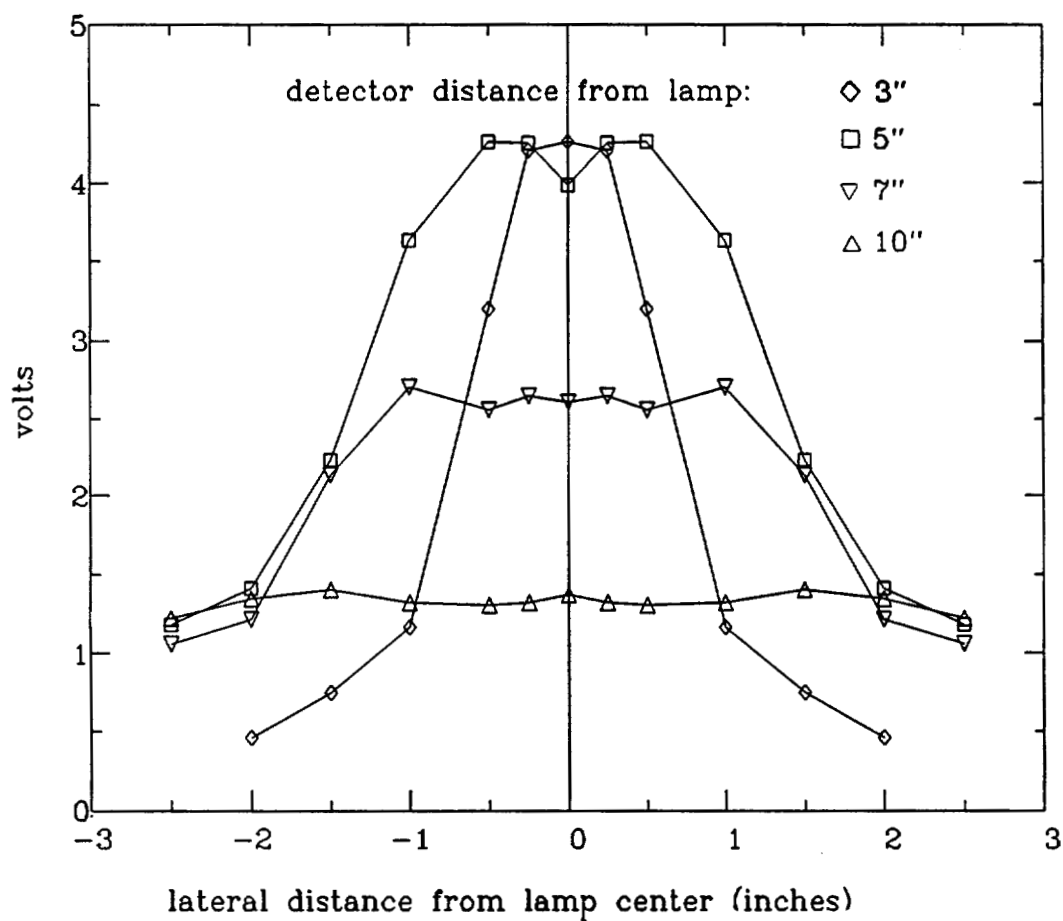


Figure 3. Lateral distribution of the beam power as a function of distance from the lamp. The lamp beam focal point occurred at 3 inches. It should be noted that the detector saturated at 4.5 volts, therefore the actual peak heights of the beam intensity were unresolved for the data taken at 3 and 5 inches.

had diverged further to from two intensity peaks separated by 2 inches. At ten inches from the bulb, the light had less intensity and the two intensity peaks were separated by 3 inches. Included in product literature from Fusion Systems, Inc., were plots of the lateral intensity of the 220 and 290 nm outputs of the lamp measured at nine inches from the lamp face. It showed two symmetric peaks separated by almost 6 inches. This confirmed this experiment's findings of a beam split; measured differences in the separation distance of the peaks resulted from differences in the experiment set-up. Therefore, the intensity profiles of the emission below 300 nm were assumed to be the same as those above 300 nm; it was known that the lamp emitted wavelengths less than 300 nm.

With the fundamental characterization of the lamp complete, the etching experiments were started. Figure 4 is a plot of the etch rates resulting from varying the temperature from 25°C to 170°C with a chamber pressure of 4 torr at a 80 sccm chlorine flow rate. Data was collected for the cases of both ultraviolet irradiated and purely thermal (no lamp irradiation) processes. Both sets of experiments demonstrated an exponential dependence upon temperature. The selections of 4 torr chamber pressure and 80 sccm flow rate were arbitrary.

Because the temperature dependence of the etch reaction appeared logarithmic in Figure 4, Arrhenius analysis was applied. The Arrhenius equation is¹⁵,

$$k = Ae^{-E/RT} \quad (1)$$

(where k = rate constant for a specific temperature, T = absolute

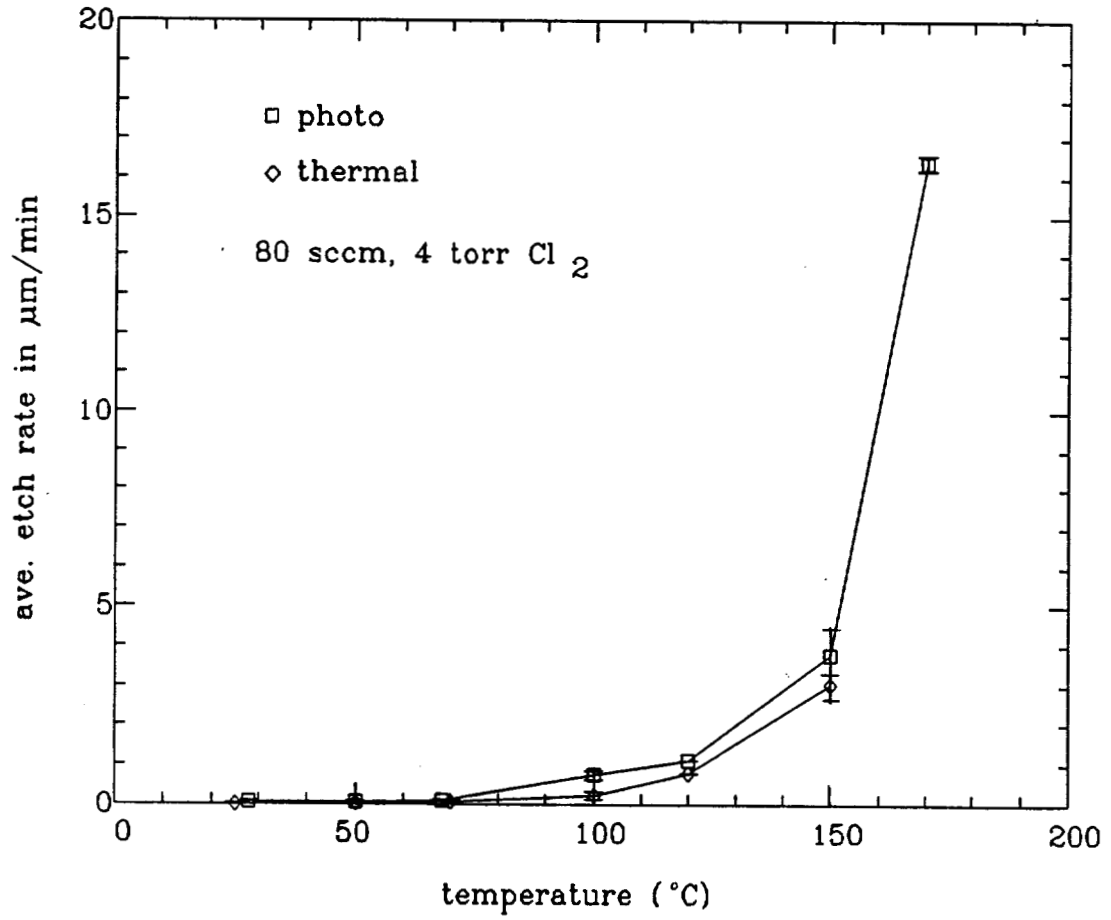


Figure 4. Temperature dependence of GaAs photoetch: experiments with 80 sccm chlorine and chamber pressure of 4 torr.

temperature, R = gas constant, and A and E are empirical constants: A = preexponential factor, E = activation energy for the reaction). Experimentally, it has been shown that the equation can hold over a fairly wide range of temperatures¹⁶ as long as the process is steady state and exhibits such dependences upon energy and temperature. In this case, no exhaustive work was done to determine whether or not the etch reaction occurred at a steady state. However, a cursory study of the dependence of the etching reaction upon etch time revealed a linear relationship. This did not demonstrate that the reaction operated at a steady state yet, the data fit the assumed Arrhenius behavior implying that the analysis was appropriate.

From an Arrhenius plot (see Figures 5, 6) of the data in Figure 4, the activation energies of the processes were calculated. For the thermal etch, this was straightforward; the slope of the plot gave an activation energy of 14.8 ± 1.5 kcal/mole. For the photo etch it appeared that the data from 25°C did not correspond to the behavior of other points. Therefore, the activation energy of the photoetch, disregarding the point at 25°C, was calculated to be 12.4 ± 1.5 kcal/mole. For comparison, Donnelly, Flamm, et. al¹⁷ etched GaAs in a chlorine plasma and found a temperature dependent process with an activation energy of 10.5 ± 0.7 kcal/mole. These results will be discussed in the following chapter.

The next set of experiments tested the pressure dependence of the etch rate. Figure 7 shows the data collected for the range of 0.2 to 8 torr Cl_2 and the temperatures of 25, 50, and 100°C. Over this range of pressure the etch rates did not evidence a linear dependence upon chlorine pressure, instead showing either saturation or a peaking behavior. This result was unexpected.

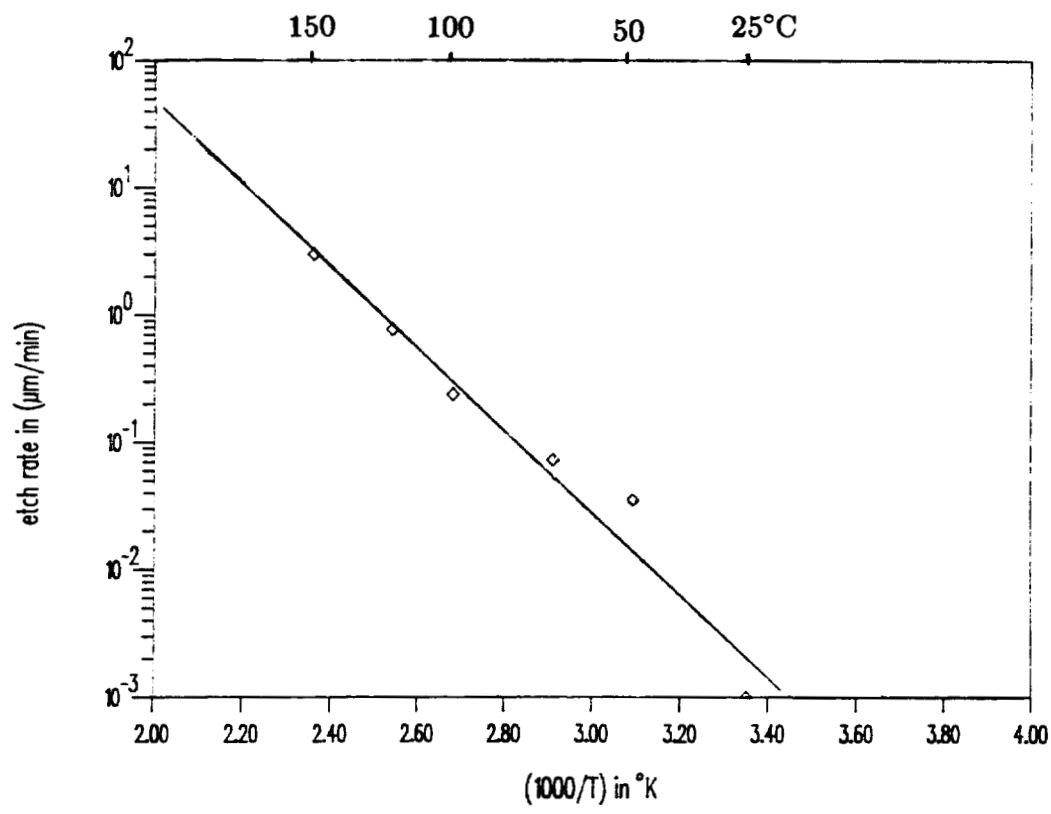


Figure 5. Arrhenius plot of 80 sccm chlorine, 4 torr, thermal etch of GaAs.

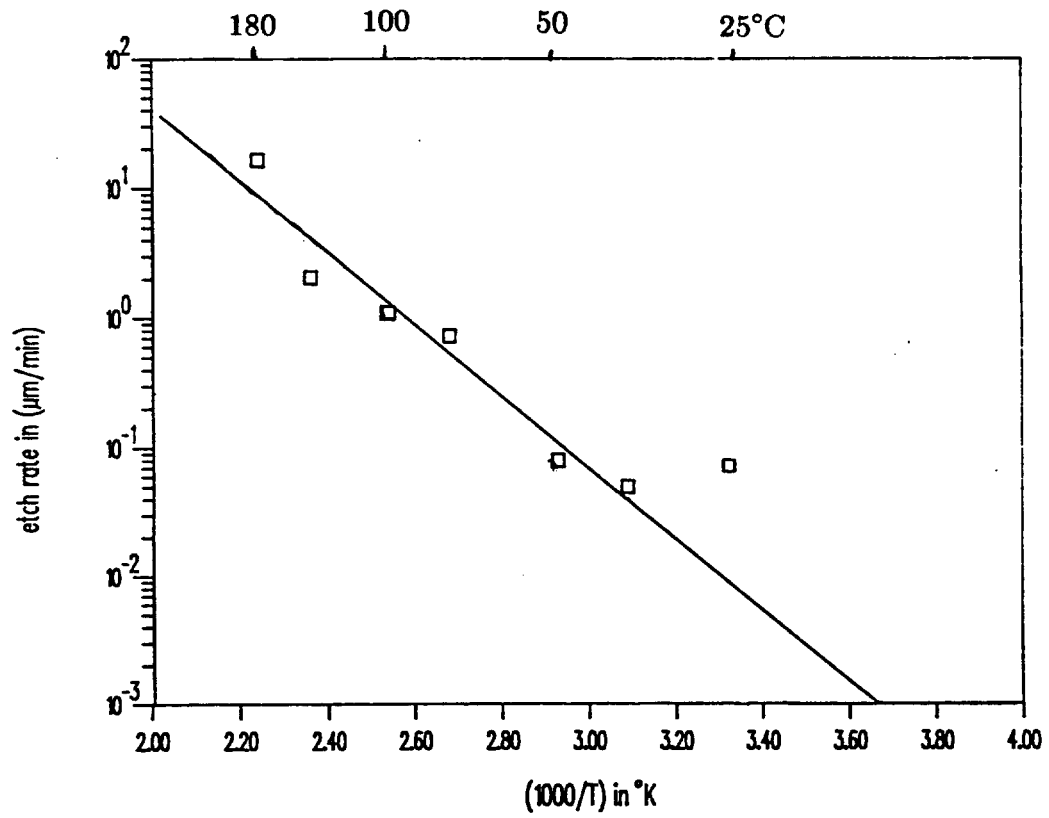


Figure 6. Arrhenius plot of 80 sccm chlorine, 4 torr, photoetch of GaAs.

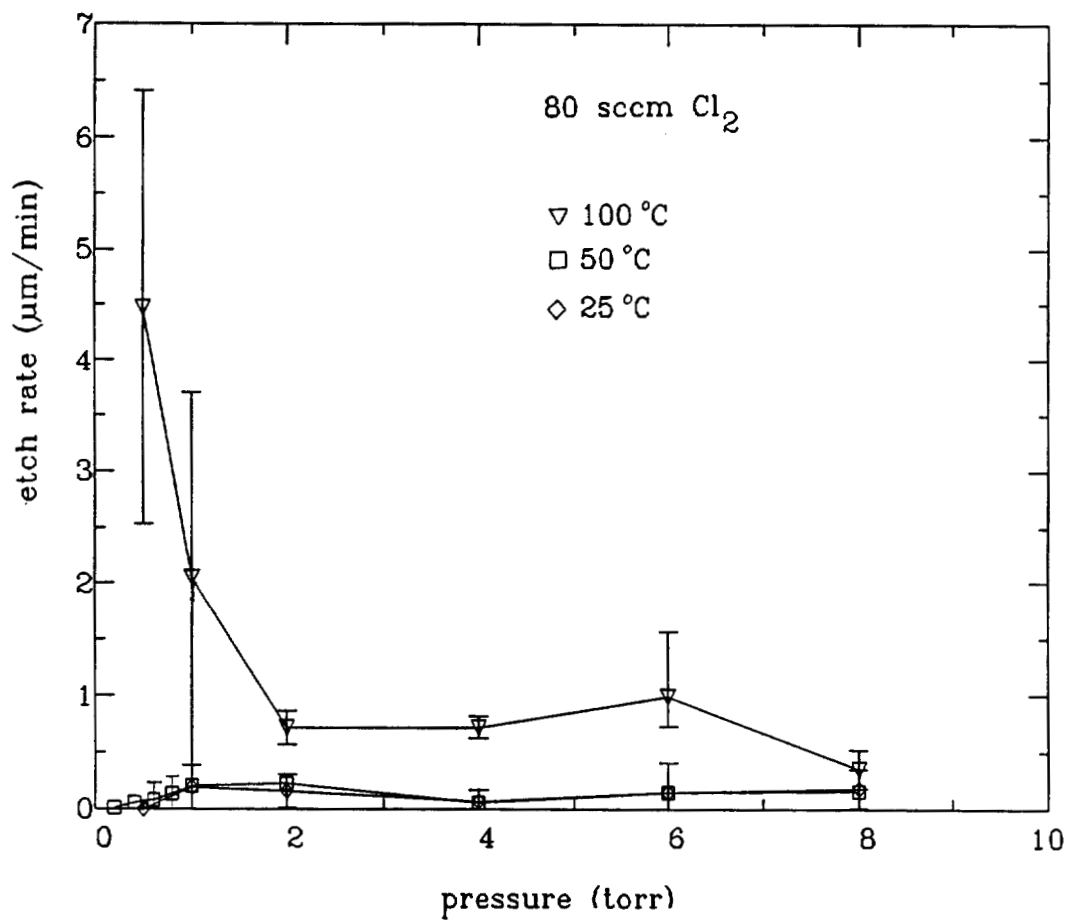


Figure 7. Dependence of GaAs photoetch upon chamber pressure of chlorine: experiments were run for constant temperatures of 25, 50, 100°C.

Ikawa¹³ etched silicon in a similar system and found a linear dependence of etch rates upon chlorine pressure over the range of 0.4 to 4.0 torr. However, his published figure had an interpolated line between the pressures of 1 and 10 torr.

It must be noted that a considerable problem with reproducibility was experienced, particularly with respect to the data taken for chamber pressures less than 1 torr and temperatures greater than or equal to 50°C. It was thought that this unpredictable behavior was due to vacuum leaks in the system and so would be more noticeable at low operating pressures. At 50°C and 0.5 torr, etch rates were recorded as great as 9 $\mu\text{m}/\text{min}$, however it was never duplicated. For calculation of the average etch rates at 50°C, then, these cases were neglected. Similar behavior, though, was noted at 100°C. At 100°C and less than 1 torr chlorine, the large variation of the data was evident in the error bars marked on Figure 7. As seen in the plot, the data from 0.5 and 1.0 torr Cl_2 had average etch rates of 4.5 and 2.1 $\mu\text{m}/\text{min}$ respectively and the error bars corresponded to an uncertainty of ± 2.0 and ± 1.5 $\mu\text{m}/\text{min}$ respectively. This was not a satisfactory result.

In order to explore the hypothesis that perhaps small concentrations of impurity gases were dramatically affecting the chlorine photoetch rate, experiments were run with small percentages of oxygen in a chlorine environment. At 25°C and a chamber pressure of 4 torr, experiments were run with 5% and 20% O_2 (see Table 1). At 50°C, experiments with 5% O_2 were run for chamber pressures of 1 and 4 torr. It was hoped that as in a plasma process³ the addition of a small amount of O_2 in a chlorine etch would enhance the etching rate. This was not evident in the data. Conversely, it appeared that

Table 1. Chemical dependence of GaAs photoetch: experiments with chlorine and oxygen as etchant gases. (*) indicates a single run.

reaction conditions	reaction gases	etch rate ($\mu\text{m}/\text{min}$)
4 torr, 25 °C	100% Cl_2	0.070 ± 0.018
	95% Cl_2 , 5% O_2	0.063 ± 0.008
	80% Cl_2 , 20% O_2	0.049 ± 0.021
	50% Cl_2 , 50% O_2	0.047 (*)
4 torr, 50 °C	100% Cl_2	0.055 ± 0.020
	95% Cl_2 , 5% O_2	0.030 (*)
1 torr, 50 °C	100% Cl_2	0.430 ± 0.113
	95% Cl_2 , 5% O_2	0.373 (*)

addition of O_2 slowed the etching reaction; most likely this occurred because the partial pressure of Cl_2 was reduced by the added gas.

Next, using Ar as a buffer gas, experiments with a chamber pressure of 7 torr and a small concentration of Cl_2 were run. These were compared with previous data for low pressure and high pressure etching with pure Cl_2 at $50^\circ C$ (see Table 2). Again, as in the experiments with O_2 as an additive, the trials showed a noticeable decrease in the etch rate compared with those experiments with only Cl_2 . This was assumed to occur directly because added gas reduced the partial pressure of the chlorine, directly reducing the amount of chlorine available to react with the substrate surface.

In an attempt to explain the etch rate variability, a study of surface oxidation of the GaAs substrates was conducted. Four samples were examined as follows: sample A was only cleaned in the usual acid bath, sample B was cleaned, mounted on the sample holder at room temperature, and the sample chamber was evacuated, sample C was cleaned, mounted on a $50^\circ C$ sample holder, and then the sample chamber was evacuated, sample D was cleaned, mounted on a $50^\circ C$ sample holder and after evacuation, the chamber was filled with 1 torr Cl_2 gas and a photoetch reaction occurred. All samples were subsequently stored in N_2 for not more than 24 hours and examined by Auger spectroscopy. Figures 8a through 8d are the results of this work. All showed the presence of Ga, As, and the surface contaminants of C, O, sometimes S, and Cl (for sample d), yet when the top 60\AA were removed from the surface (done by Ar sputter etching during Auger analysis), only signals from G and As remained in all cases. This demonstrated that all the contaminants penetrated no farther than 60\AA . It remained unknown exactly how

Table 2. Chemical dependence of GaAs photoetch: experiments
with chlorine and argon as etchant gases.

reaction conditions	reaction gases	etch rate ($\mu\text{m}/\text{min}$)
7 torr, 50 °C	20% Cl_2 , 80% Ar	0.031 ± 0.007
	8% Cl_2 , 92% Ar	0.023 ± 0.003
1 torr, 50 °C	100% Cl_2	0.430 ± 0.113
6 torr, 50 °C	100% Cl_2	0.153 ± 0.029

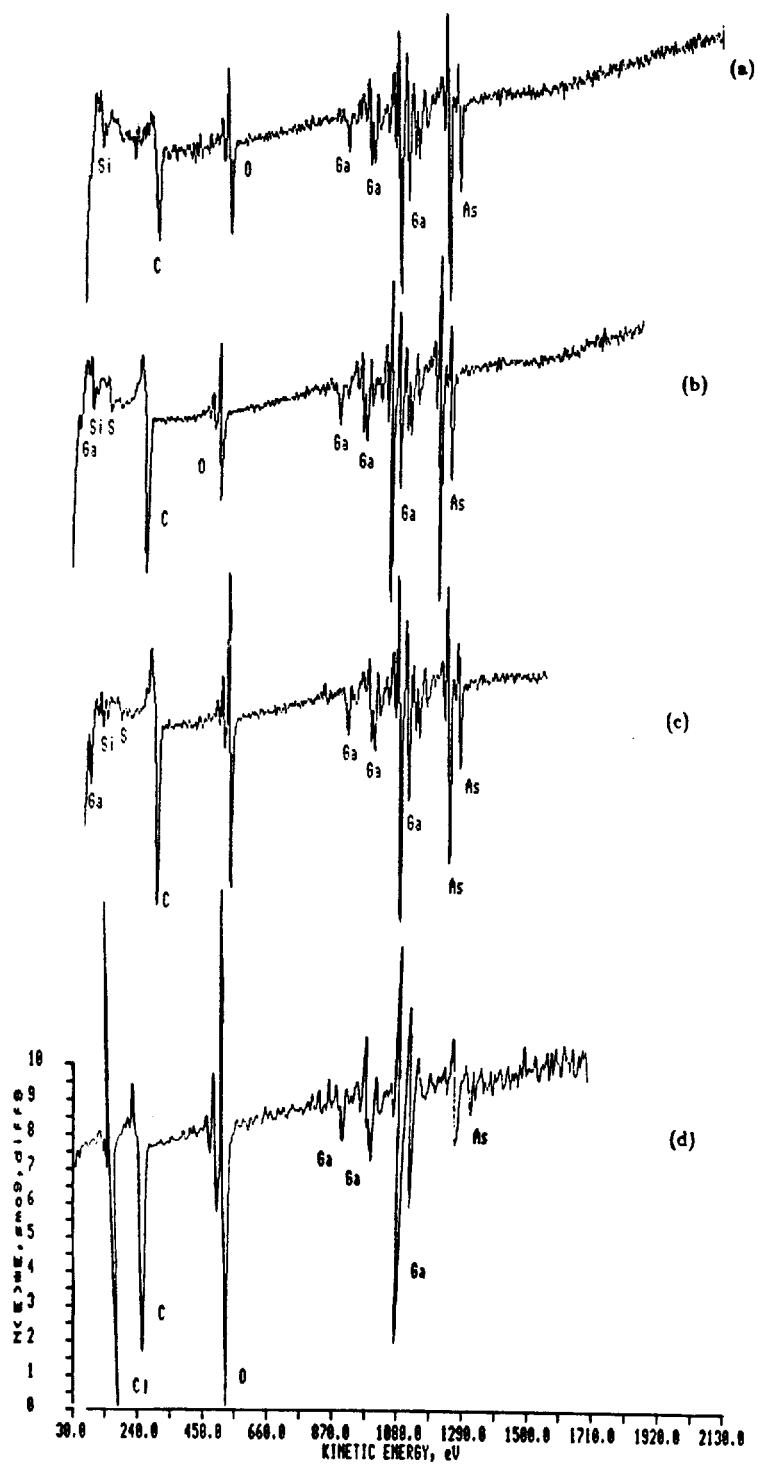


Figure 8. Auger spectroscopic analysis of surfaces of GaAs substrates (A,B,C,D) in progressive stages of an experimental run. See text for substrate conditions.

far the contaminants penetrated the surface. Closer examination of the Auger spectra revealed that the proportions of surface elements changed during the experiment. After experimental etching there was seen to be a large increase in the Ga/As ratio and a noticeable increase in the O/C ratio. The larger Ga/As ratio is interesting since although the gallium chlorides have been found to be less volatile than the arsenic chlorides⁴ researchers^{4,17} have reported that it is the formation and desorption of the gallium chlorides which are rate limiting. The larger O/C ratio was not quite as meaningful; it was unclear what role, if any, that oxygen played in the etching reaction.

The next variable tested was the intensity dependence of the photoetch. Rather than increasing the distance between the lamp and the substrate surface to reduce the incident intensity of the lamp, screen mesh was placed in the light path to attenuate the radiation. Several different stainless steel mesh screens were used. Screen 1 transmitted 80% of incident radiation, screen 2 transmitted 43% of incident radiation, and combination of both screens 1 and 2 allowed transmission of 36% of incident radiation. For a substrate temperature of 50°C, the etch rates as a function of intensity were collected (see Figure 9). Uncertainty in the points was rather large, yet the plotted data did not show a linear relationship. The reason for the observed behavior cannot be explained at this time.

The last variable considered was the effect of changes in the type of GaAs substrate. Experiments were run to compare any differences between Horizontal-Bridgeman grown (HB), $\langle 100 \rangle$, n-type GaAs with a doping density of approximately 10^{18} cm^{-3} and a liquid encapsulated Czochralski (LEC) grown, $\langle 100 \rangle$ GaAs with an unintentional background n-type doping den-

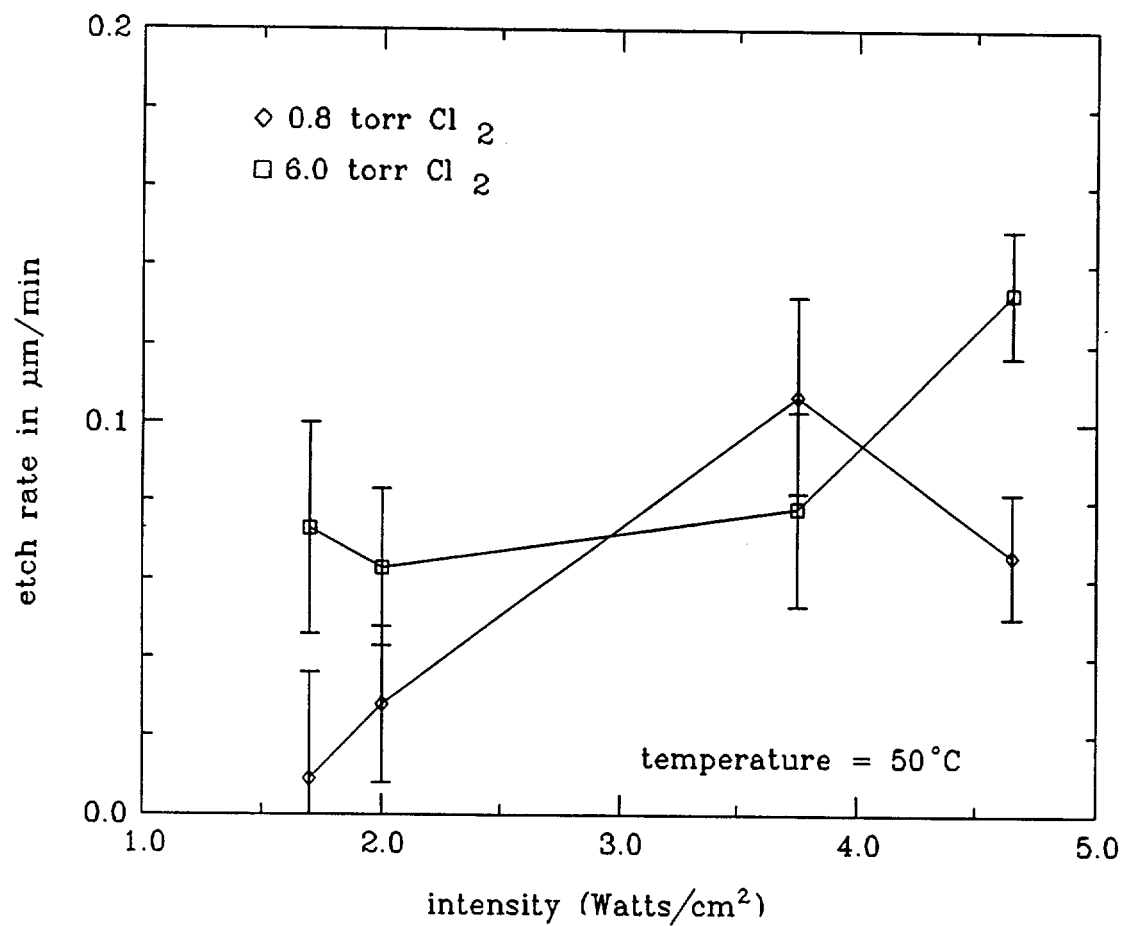


Figure 9. Photon dependence of GaAs photoetch: experiments at 50°C and chamber pressures of 0.8 and 6.0 torr chlorine.

sity estimated to be $<10^{17} \text{ cm}^{-3}$. Table 3 lists the results of this work. The more highly doped HB wafers did etch faster than the purer LEC GaAs wafers; this was expected since Schwartz and Schaible¹⁸ in their work with silicon found that more highly doped substrates had faster etch rates. This occurs because impurities in the lattice structure allow easier chemical attack.

Another tool used to gain a better understanding of the photoetch mechanism was the scanning electron microscope (SEM). Scanning electron micrographs were taken of representative experiment samples to determine the characteristics of the etched profile. This work revealed that only two types of profiles resulted. Figure 10 shows the semi-anisotropic, smooth-walled profile of all low speed etches - etch rates less than $0.5 \mu\text{m}/\text{min}$. Figure 11 shows the semi-anisotropic, crystallographically undercut etch profile of all high speed etches - etch rates greater than $0.5 \mu\text{m}/\text{min}$.

One interesting feature of the low speed etches was the presence of an etch trench parallel to all edges of the silicon nitride mask (see Figure 12). Its existence did not appear to be chemical in nature and recently was explained by Mayumi, Fujiwara, et. al.¹⁹ By annealing the substrate before etching, they were able to eliminate the feature. Therefore, it was concluded that the surface stress of the deposited mask caused preferential etching along the mask borders.

Table 3. Substrate effect in GaAs photoetch: experiments with Horizontal-Bridgeman (HB) grown, $\langle 100 \rangle$, n-type GaAs of doping density 10^{18} cm^{-3} , and liquid encapsulated Czochralski (LEC) grown, $\langle 100 \rangle$ GaAs with an n-type doping density of 10^{17} cm^{-3} .

reaction conditions	GaAs growth method	etch rate ($\mu\text{m}/\text{min}$)
0.8 torr, 50 °C	LEC	0.066 ± 0.037
	HB	0.144 ± 0.058
1 torr, 50 °C	LEC	0.095
	HB	0.205 ± 0.082
6 torr, 50 °C	LEC	0.133 ± 0.016
	HB	0.153 ± 0.029

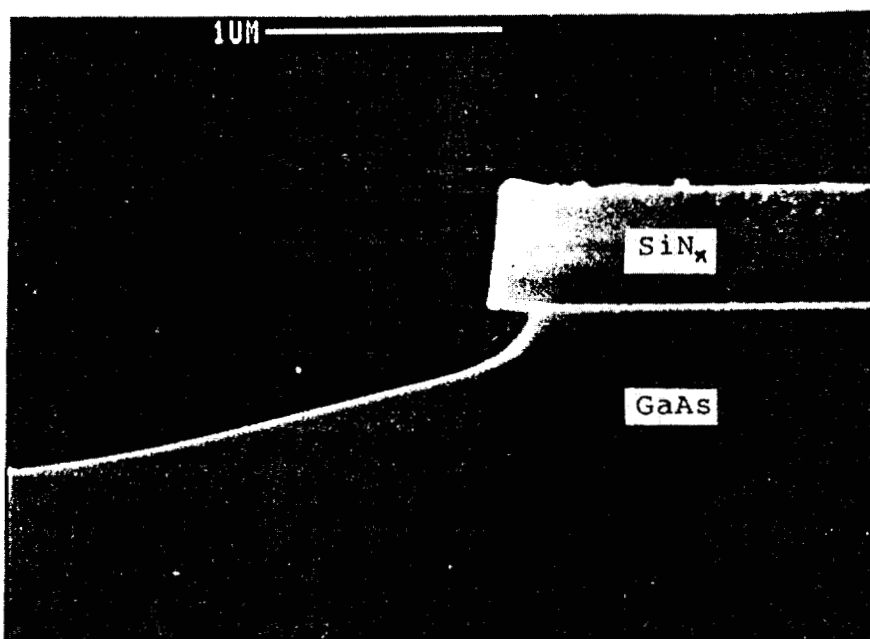


Figure 10. SEM micrograph showing the smooth-walled profile of low speed etches.

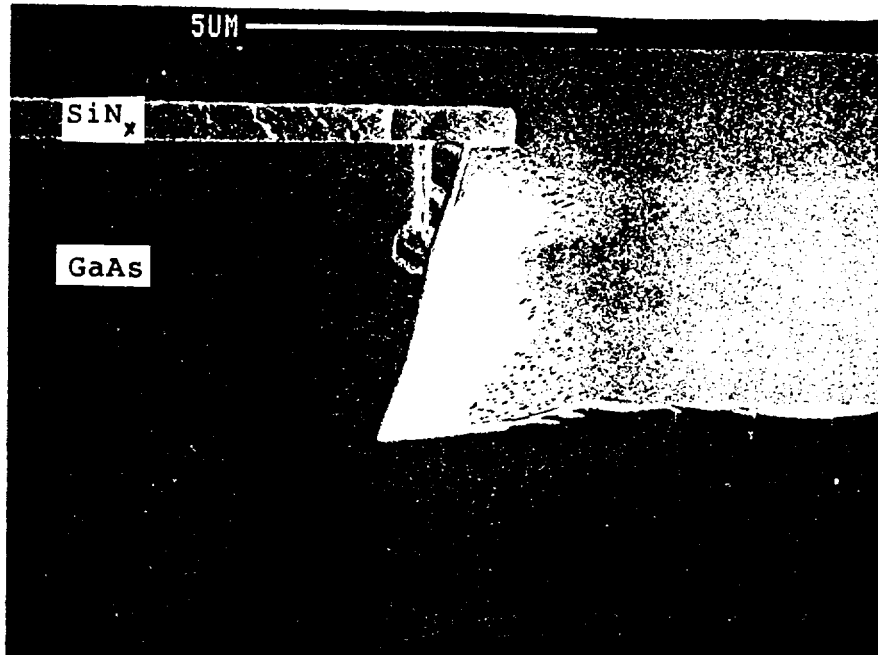


Figure 11. SEM micrograph showing the crystallographic etching of high speed etches.

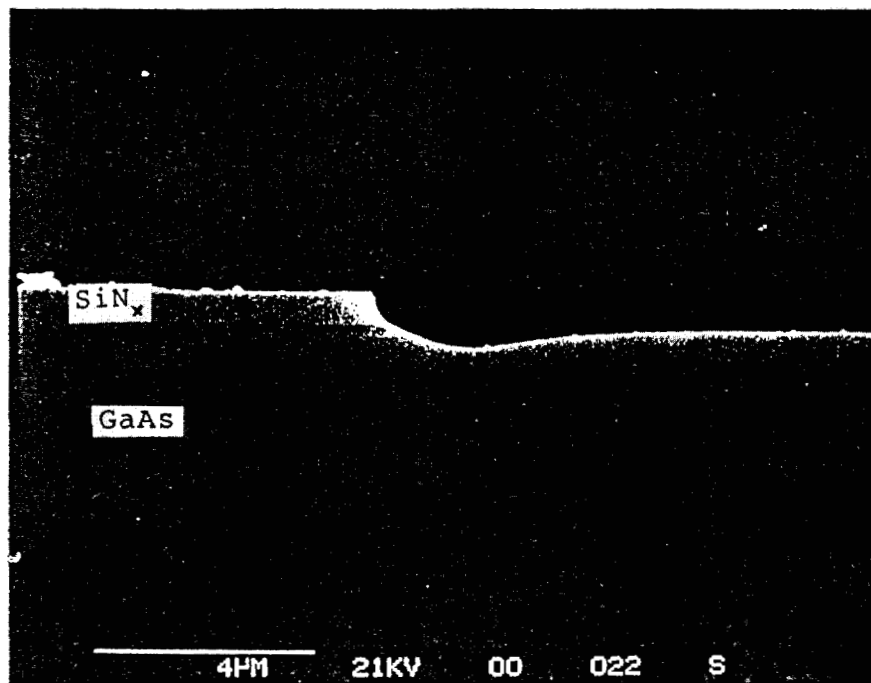


Figure 12. SEM micrograph showing the etch trenching feature parallel to the edge of the GaAs mask.

IV. DISCUSSION

With the collection of data complete, the challenge remained to explain the results and to suggest a mechanism for the etch reaction.

First considering the etchant gas, the Cl-Cl bond has a binding energy of 2.47 eV and can be photolyzed at 3471Å.²⁰ Therefore, from Figure 2, it was clear that one photon from the lamp would have sufficient energy to dissociate the chlorine molecule.



However because the chlorine gas absorbed the lamp emission so strongly, the actual photon intensity reaching the substrate surface for various pressures of chlorine needed to be determined. The power meter was not used for this as the detector head was too bulky to fit in the sample chamber. Therefore a photovoltaic, Si photodiode with a measurement range from 185 nm to 870 nm was placed where samples were mounted. With the system not under vacuum and at atmosphere, the sample surface was measured to receive about 3 Watts/cm² from the lamp. No measurements were made of the photon intensity at the substrate surface when the sample chamber was filled with chlorine gas.

From a plot of the absorption coefficients of chlorine gas as a function of wavelength in Noyes, Jr. and Leighton²¹ it was possible to calculate the ratio of incident lamp emission reaching the substrate surface. Table 4 lists the transmission ratio for the range of pressures from 0.5 to 8.0 torr assuming incidence of a 350 nm photon. The wavelength of 350 nm was selected since

Table 4. Calculated values for the ratio of transmitted lamp intensity reaching the substrate surface for a chlorine pressure range of 0.5 to 8 torr. Figures were derived using a path distance of 3 cm and assuming incidence of a 350 nm photon.

Cl_2 pressure (torr)	Cl_2 concentration (mole/liter)	I/I_0
0.5	2.37×10^{-9}	0.99
1.0	4.69×10^{-9}	0.99
2.0	9.38×10^{-9}	0.99
4.0	1.87×10^{-8}	0.99
6.0	2.80×10^{-8}	0.99
8.0	3.74×10^{-8}	0.99

it is the wavelength of maximum absorption by Cl_2 (see Figure 2). While the transmitted intensity does decrease slightly for increasing pressures of chlorine, at 8 torr, still 99% of the original intensity is transmitted. This still is sufficient power to activate the chlorine species, therefore it could be assumed that for all experiments, activated Cl_2 species were present at the reaction site.

Attempting to model the possible behavior of the gas, a crude picture was obtained by calculating the mean free path and residence time of Cl_2 . Using the approximations from Chapman²³ of an atomic diameter of 3.6Å, a collision area of $2.8 \times 10^{-15} \text{ cm}^2$, and a volume per molecule of $3.54 \times 10^{-13} \text{ cm}^3$ at a pressure of 1 mtorr (at a temperature of 300°K) the mean free path of Cl_2 could be determined from,

$$\left[\text{collision area} \right] \times \left[\text{mean free path} \right] = \left[\text{volume per molecule} \right]. \quad (3)$$

Table 5 lists these values for pressures of 0.5 to 6.0 torr. It is important to note that for higher chamber pressures, the chlorine not already at the substrate surface would not be able to travel to the surface without collision. This implies that distant activated chlorine species would most likely be deactivated by collision before reaching the reaction surface. Therefore the figures suggest that for higher pressure etching reactions, chlorine radicals formed near the reaction surface are the most important.

In a separate calculation, the residence time of the chlorine gas in the reaction chamber was determined. Again using an equation from Chapman,

$$\text{residence time} = \frac{\text{chamber pressure} \cdot \text{chamber volume}}{\text{flow rate}} \quad (4)$$

Table 5. Calculated values for the volume per molecule and mean free path of Cl_2 for varying pressures assuming a volume per molecule of 3.45×10^{-13} at a pressure of 1 mtorr.

pressure (torr)	volume per molecule (cm^3)	mean free path of Cl_2 (cm)
0.5	7.0×10^{-16}	0.250
1.0	3.5×10^{-16}	0.126
2.0	1.7×10^{-16}	0.063
4.0	8.8×10^{-17}	0.031
6.0	5.9×10^{-17}	0.021

the values in Table 6 were derived. However, the fact that individual chlorine molecules spent more time in the reaction chamber before being pumped out as the chamber pressure increased did not necessarily counteract the fact that the mean free path was simultaneously shrinking. Therefore, activated chlorine species which are proposed here as the more active etchants of GaAs would be deexcited by collision or removed by recombination more rapidly as the pressure increased. This suggested that there might be a pressure where the etch rate reached a maximum - at lower chamber pressures, a small pressure increase would increase the etch rate as the concentration of the reactant Cl_2 increased, and then at higher chamber pressures, a pressure increase would decrease the etch rate as the chlorine mean free path decreased.

Examining the data from the chlorine pressure versus etch rate study presented in Figure 7, at temperatures below 100°C the etch reaction rates increased as the pressure of Cl_2 increased from zero. These rates all peaked at about 2 torr Cl_2 and then either levelled off or declined to a final etch rate of approximately $0.5 \mu\text{m}/\text{min}$ for all Cl_2 pressures greater than 6 torr. This behavior indicates that until a chamber pressure of 2 torr Cl_2 is reached, the amount of available Cl_2 is the etch reaction bottleneck. After pressures of 2 torr Cl_2 have been exceeded, though, there is an obvious deactivation of the etch conditions. This could result from either deactivation of the Cl_x species due to recombination or from the effect of a reduced intensity of light striking the substrate surface.

Considering the first explanation, it was seen in Table 5 that as the Cl_2 pressure increased from 0.5 to 4.0 torr, there was a corresponding tenfold

Table 6. Calculated values for the residence time of Cl_2 using the total chamber volume of 2.87 liters, for varying chamber pressures.

pressure (torr)	residence time (sec)
0.5	0.01
1.0	0.03
2.0	0.07
4.0	0.14
6.0	0.21

decrease in the expected Cl_2 mean free path. However, this calculation was only for Cl_2 and not for the activated Cl_2 species. Since activated chlorine species could also undergo deexcitation and recombination, the actual mean free path of activated Cl_2 could be much shorter. Therefore the idea that at increased pressures of Cl_2 there would be fewer available activated species seemed accurate.

Considering the second explanation, it seems unlikely that a lessened light intensity would have such a pronounced effect. As listed in Table 4, even at a chamber pressure of 8.0 torr Cl_2 , the substrate surface still receives 99% of the original lamp radiation. Such a slight decrease in light intensity would not be expected to have a discernible effect upon the etch reaction.

The results of the gas dependence work (see Tables 1 and 2) appear to confirm the hypothesis that the decrease in etch reaction rates with increasing Cl_2 pressures is due to the deactivation of the Cl_2 species. When the chamber pressure was due to both Cl_2 and O_2 , the etch rate always was less than that resulting from pure Cl_2 , implying that less available activated Cl_2 directly affected the GaAs etch rate. Similarly, when Cl_2 and Ar were mixed in the chamber, again there was a marked decrease in the etch rate.

It was intended that the Auger surface analysis would resolve the issue of contaminants. As seen in Figure 8, there was surface oxidation present at all stages of the experiment. However, without knowing the depth of surface oxidation penetration and being unable to remove it, it was unclear how this oxidation affected the etch reaction. It was assumed, then, that substrate oxidation was an experimental constant.

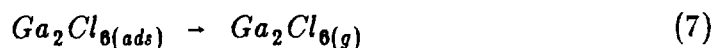
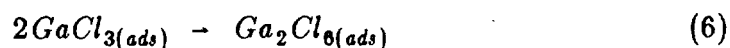
After considering the gas dependence of the etching, its temperature dependence was explored. As mentioned in the previous section, an Arrhenius analysis of these data was appropriate. So what did the computed activation energies of 12.4 ± 1.5 kcal/mole and 14.8 ± 1.5 kcal/mole for the photo and thermal etches respectively indicate about the etch mechanism?

Examining the data presented in Figures 5 and 6, it was apparent that there was a lot of similarity in the data - between thermal and photoetching - especially for the higher temperatures. Since the activation energies for the separate etch reactions in that temperature range were within the error of the measurement, they were assumed to be the same and hence the fundamental etch mechanism was the same for both thermal and photoetching in that region. For those higher temperatures, then, the dominant process of the etching clearly was thermal or desorptive.

However, at lower temperatures (at 25°C) etching data did not exhibit the Arrhenius behavior of the other experiments (see Figure 6). It was assumed that in addition to any thermal process, there was a significant photoetch component to the 25°C etching. Apparently, this photoetch mechanism was dominated by the presence of the thermal etching which occurred at all higher temperatures.

Comparing this conclusion with other researchers' results, Donnelly, Flamm, et. al¹⁷, etched GaAs in a chlorine plasma at 0.3 torr and found a temperature dependent etch resulting in an activation energy of 10.5 ± 0.7 kcal/mole. (As seen in Figure 5, the thermal etch of GaAs in this experiment was 14.8 ± 1.5 kcal/mole.) Although their calculated figure for the activation energy of GaAs etching was close to the latent heat of vaporiza-

tion of $GaCl_3$ (12 kcal/mole)¹⁷, they found a large discrepancy between the calculated evaporation rate and the observed etch rate. This led to the conclusion that adsorbed $GaCl_3$ molecules did not evaporate directly but formed a dimer, Ga_2Cl_6 , which evaporated. Therefore it would be the escape of $Ga_2Cl_6(g)$ from the substrate surface which would be rate-limiting and not the escape of $GaCl_3(g)$. This proposed etch reaction is,



where it should be noted that the escape of $AsCl_3(g)$ is known to present no complications⁴. Conversely, the removal of $GaCl_3(ads)$ from the surface is crucial.

Using the data shown in Figure 7, additional Arrhenius plots of the photoetch rate versus $1000/T$ were created for different chamber pressures of chlorine (see Figure 13). Table 7 lists the calculated activation energies for the photoetch of GaAs at various pressures of chlorine. Since the figures were generated from three point plots, it is unclear how reliable they are yet, they still provide an opportunity for speculation. This data demonstrates that the activation energy of the etch reaction is dependent upon the pressure of chlorine. This is a puzzling conclusion since earlier data demonstrated that for all etches $>25^\circ C$, there was a dominant temperature dependent mechanism - the data fit well in an Arrhenius analysis. However, the Arrhenius equation does not include any variable for pressure (see equation

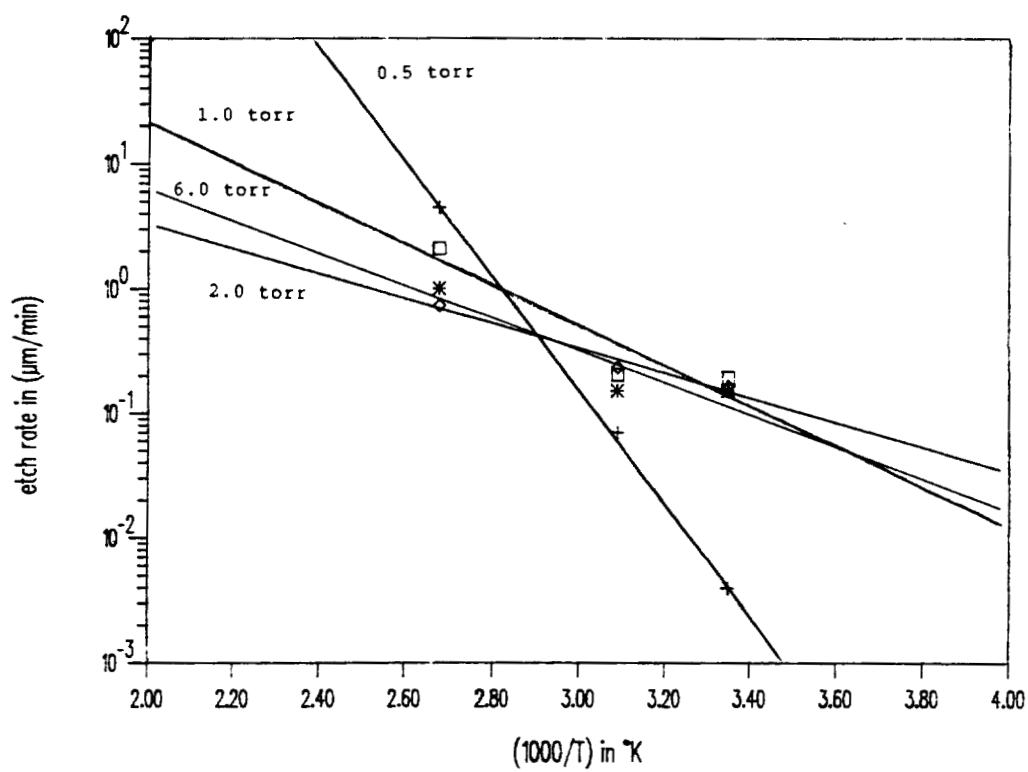


Figure 13. Arrhenius plots of the photoetch rate versus $1000/T$ (in degrees Kelvin) for the following chamber pressures of chlorine: 0.5, 1.0, 2.0, 6.0 torr.

Table 7. Activation energies of GaAs photoetch for a range of chlorine pressures, derived from Arrhenius plots of the etch rate versus $1000/T$ in degrees Kelvin.

pressure of Cl_2 (torr)	activation energy (kcal/mole)
0.5	20.5 ± 0.6
1.0	7.3 ± 2.8
2.0	4.5 ± 0.6
4.0	12.4 ± 1.5
6.0	5.8 ± 2.3

1). If this data is correct, it could mean that changes in the experiment pressure either open or close alternate pathways of the reaction. It was unclear if this actually occurred.

In conclusion, examination of the data uncovered several possible contributing factors to the etch reaction. The etch mechanism is rate-limited by a thermal process for all temperatures $\geq 25^{\circ}\text{C}$; however, the reaction rate can be increased at all temperatures by irradiation with uv. The etch reaction only appears to have a substantial photochemical component when conducted at or below 25°C . Auger studies and Arrhenius analysis of the etch reaction gave strong indications that the formation and desorption of gallium chlorides were crucial to the etch reaction. And lastly, the gas studies and pressure dependence experiments demonstrated that the etch reaction also appears to be controlled by gas phase species of Cl_2 .

V. CONCLUSION

Using a high power uv lamp, a low pressure system and chlorine gas, a new method of photoetching GaAs was developed. By varying the pressure of Cl_2 from 0.5 to 8.0 torr and the temperature of the n-type, $\langle 100 \rangle$ GaAs substrate from 25 to 170°C, etch rates were obtained from 10 Å/min to 10 μm/min. Etch rates were found to be exponentially dependent upon temperature except for temperatures $\leq 25^\circ\text{C}$ where there was evidence of some photochemical etching. The etch reaction also was observed to depend upon the pressure of Cl_2 with a maximum rate at about 2 torr Cl_2 . This pressure dependence was proposed to be related to changes in the chlorine mean free path (for pressures greater than 4 torr). There was good repeatability of data for the fast etch rates ($> 1 \mu\text{m}/\text{min}$); however, these etch profiles were found to be crystallographic and were produced by a dominant thermal etch reaction. The slower etch rates ($< 1 \mu\text{m}/\text{min}$) were difficult to reproduce and this problem was not resolved.

One goal of this thesis was to find a photochemical and low damage etch process. Were more work to be done, it would be interesting to explore the low temperature ($< 25^\circ\text{C}$) Cl_2 etching since this was the only region where a photochemical mechanism was observed. However, it was exactly this region where the etch reaction was found to be inconsistent and highly variable. Contaminants did not appear to contribute to the non-reproducibility; however, the desorption of $GaCl_3$ appeared to be crucial. Therefore at lower temperatures and pressures, a photochemical mechanism was encouraged but the substrate surface could not desorb the chlorides well. Heating the

substrate to aid in the desorption, unfortunately also triggered a thermal etch reaction. More work would need to be done to overcome this limit to the photoetch process.

References

1. S. Ghandhi, *VLSI Fabrication Principles*, pp. 499-501, John Wiley & Sons, New York, 1983.
2. S. Pang, "Dry etching induced damage in Si and GaAs," *Solid State Tech.*, pp. 249-256, April 1984.
3. S. Semura, H. Saitoh, "Hydrogen mixing effects on reactive ion etching of GaAs in chlorine containing gases," *J. Vac. Sci. Technol. A*, vol. 2(2), pp. 474-476, Apr./June 1984.
4. M. Balooch, D. Olander, "The thermal and ion-assisted reactions of GaAs (100) with molecular chlorine," *J. Vac. Sci. Technol. B*, vol. 4(4), pp. 794-805, Jul/Aug 1986.
5. R. Osgood, "Laser microchemistry and its applications to electron-device fabrication," *Ann. Rev. Phys. Chem.*, vol. 34, pp. 77-101, 1983.
6. G. Loper, M. Tabat, "UV laser-induced radical-etching for microelectronic processing," *SPIE: Laser assisted deposition, etching and doping*, vol. 459, pp. 121-127, 1984.
7. C. Ashby, R. Biefeld, "Composition selective photochemical etching of compound semiconductors," *Appl. Phys. Lett.*, vol. 47(1), pp. 62-63, July 1, 1985.
8. A. Tucker, M. Birnbaum, "Laser chemical etching of vias in GaAs," *IEEE Electron Dev. Lett.*, vol. EDL-4(2), pp. 39-41, Feb. 1983.
9. D. Ehrlich, R. Osgood, T. Deutsch, "Laser-induced microscopic etching of GaAs and InP," *Appl. Phys. Lett.*, vol. 36(8), pp. 698-700, April 15, 1980.

10. Y. Horiike, M. Sekine, K. Horioka, T. Ariada, H. Okano, "Photon-excited dry etching for VLSI's," *Extended Abstracts of 16th Conference on Solid State Devices and Materials*, pp. 441-446, Kobe, 1984.
11. P. Brewer, S. Halle, R. Osgood, "Photon-assisted dry etching of GaAs," *Appl. Phys. Lett.*, vol. 45(4), pp. 475-477, Aug. 15 1984.
12. C. Ashby, "Doping level selective photochemical dry etching of GaAs," *Appl. Phys. Lett.*, vol. 46(8), pp. 752-754, 1985.
13. E. Ikawa, S. Sugito, Y. Kurogi, "Silicon photo etching in Cl₂ gas using a high power Hg lamp," *Surf. Sci.*, vol. 183, pp. 276-288, 1987.
14. H. Okabe, *Photochemistry of Small Molecules*, pp. 184-185, 299-308, John Wiley & Sons, New York, 1978.
15. S. Benson, *Thermochemical Kinetics, 2nd. ed.*, pp. 10-14, John Wiley & Sons, New York, 1976.
16. S. Benson, *The Foundations of Chemical Kinetics*, pp. 66-67, Mc Graw-Hill Book Comp., Inc., New York, 1960.
17. V. Donnelly, D. Flamm, C. Tu, D. Ibbotson, "Temperature dependence of InP and GaAs etching in a chlorine plasma," *J. Electrochem. Soc.*, vol. 129(11), pp. 2533-2537, Nov. 1982.
18. G. Schwartz, P. Schaible, "The effects of arsenic doping in reactive ion etching of silicon in chlorinated plasmas," *J. Electrochem. Soc.: Solid-State Science and Technology*, vol. 130(9), pp. 1898-1905, Sept. 1983.
19. S. Mayumi, K. Fujiwara, S. Nishida, S. Ueda, M. Inoue, "Etch-back planarization technique for multilevel metallization," *Jap. J. Appl. Phys.*, vol. 27(2), pp. 280-286, Feb. 1988.

20. G. Busch, R. Mahoney, R. Morse, K. Wilson, "Translational spectroscopy: Cl₂ photodissociation," *J. Chem. Phys.*, vol. 51(1), pp. 449-450, July 1, 1969.
21. W. Noyes, P. Leighton, *The Photochemistry of Gases*, p. 264, Dover Publications, Inc., New York, 1941.
22. B. Chapman, *Glow Discharge Processes*, pp. 1-19, John Wiley & Sons, New York, 1980.

BIOGRAPHICAL NOTE

The author was born in Madison, Wisconsin, on January 21, 1964. She attended Mount Holyoke College in Massachusetts and during her last year was awarded the Skinner and Dana fellowships for her work with hydrogen ion implantation - a cooperative project between Stanford University and Mount Holyoke College. She was graduated magna cum laude in May of 1986, receiving the Bachelor of Arts degree.

The author began her studies at the Oregon Graduate Center in September, 1986. In September of 1988, the author enrolled in the entering medical school class of the Oregon Health Sciences University. In July, 1989, she completed the requirements for the degree of Master of Science in Applied Physics. At this writing, the author remains enrolled at the Oregon Health Sciences University and expects to be graduated with her class, receiving the Doctor of Medicine degree in 1992.